



The Arcminute Microkelvin Imager

K. Grainge

Cavendish Laboratory, JJ Thomson Avenue, Cambridge CB3 0HE, United Kingdom

Abstract. The Arcminute Microkelvin Imager is a dual array interferometer designed specifically to survey for galaxy clusters through detecting their Sunyaev-Zel'dovich signatures on the microwave background. Construction of the Small Array is now complete and commissioning observations have mapped several clusters. The Large Array is required to remove the effects of confusing radio sources and will allow deep, blind surveys for clusters.

1. Motivation for a Galaxy Cluster Survey

Clusters of galaxies are the most massive collapsed objects in the Universe. They are sensitive probes of structure formation, both in the linear regime of growth and when merging, shocking and gradual virialisation occur. Determining the evolution of clusters, their mass function and structures is therefore of basic importance. A population of clusters at $z > 1$ is now known to exist (Rosati et al. 2002). However, more data and in particular an unbiased cluster survey are needed to understand cluster formation and early evolution at these redshifts. Optical and X-ray observations suffer from confusion and from a bias towards concentration of mass; another approach is to survey for clusters through detecting their Sunyaev-Zel'dovich (S-Z) effect and several dedicated SZ survey instruments are now being built (see e.g. Mohr et al 2000; Lo 2002; Mohr et al. 2003; Kosowsky 2003; Kneissl et al. 2001).

2. The Sunyaev-Zel'dovich Effect

The S-Z effect (Sunyaev & Zel'dovich 1972) is a secondary anisotropy on the Cosmic Microwave Background (CMB) radiation due to inverse-Compton scattering of CMB photons by hot plasma in the gravitational potential of a cluster of galaxies. The S-Z effect has been detected by a number of different groups using a variety of observing techniques (e.g. Birkinshaw & Hughes 1994; Myers et al. 1997; Reese et al. 2000; Komatsu et al. 1999; Pointecouteau et al. 1999; Holzapfel et al. 1997; Grainge et al. 1993; Lancaster et al. 2005; Udomprasert et al. 2004. See e.g. Birkinshaw 1999 or Carlstrom et al. 2002 for a full review).

CMB photons are up-scattered in energy with the result that, at frequencies below 220 GHz, one sees a decrease in the CMB temperature towards the cluster. In the Rayleigh-Jeans regime this dip is given by

$$\Delta T = -2yT_{\text{cmb}}, \quad (1)$$

where y is the Comptonisation parameter

$$y = \int n_e \sigma_T \frac{kT_e}{m_e c^2} dl. \quad (2)$$

Importantly the intensity of the S-Z effect is independent of redshift. The reason for this is that in such a Compton scattering process, the power lost by the electrons and given to the CMB photons is proportional to the energy density of the incident CMB radiation which is proportional to $(1+z)^4$; this exactly cancels out the cosmological drop in surface brightness proportional to $(1+z)^{-4}$.

S-Z surveys for clusters have long been advocated (Korolev et al. 1986; Bond & Myers 1991; Bartlett & Silk 1994) and it is now widely recognised that such surveys are key measurements for cosmology. Such a method has several key advantages. Firstly, because the surface brightness of the S-Z effect does not decrease with redshift, one can detect clusters of galaxies all the way back to their epoch of formation. Further, the measured total flux density of the S-Z effect from a cluster is very closely related to its mass, which is precisely the quantity we wish to observe. This can be seen from the following. The brightness temperature of the S-Z effect is proportional to the integral of the gas pressure along the line of sight,

$$\Delta T_{\text{SZ}} \propto \int nT dl, \quad (3)$$

while the total flux density is proportional to the integral of the surface brightness over solid angle

$$\Delta S_{\text{SZ}} \propto \int \Delta T_{\text{SZ}} d\Omega. \quad (4)$$

The flux density is therefore proportional to the total thermal energy in the cluster

$$\Delta S_{\text{SZ}} \propto D_A^{-2} \int nT dV, \quad (5)$$

where D_A is the angular size distance. Because of the flatness of the angular size vs redshift relation, D_A is only weakly dependent on redshift. The total S-Z flux density from a cluster is thus a measure of its mass, since in gravitational collapse models the thermal energy is simply the gravitational potential energy of the cluster (assuming full virialisation). An S-Z survey that is complete down to a particular S-Z flux density limit would therefore be complete down to a cluster mass limit *with no limiting*



Fig. 1. The AMI Small arrays.



Fig. 2. The AMI Large array.

redshift and largely independent of the detailed cluster astrophysics. A principal aim of the AMI project is to carry out this survey work (Kneissl et al. 2001).

3. AMI Hardware

AMI (Jones 2002) comprises two synthesis arrays (shown in Fig. 1 and Fig. 2), sited at Lord's Bridge, Cambridge. The Small Array consists of ten 3.7-m antennas situated inside a 30×40 -m, 4.5-m high metal enclosure. The Large Array is an upgrade to the Ryle Telescope (RT) with all eight 13-m antennas now placed in a new 2-dimensional compact configuration. The dual array design gives AMI good temperature sensitivity over a very large range of angular scales, as well as the high flux sensitivity needed to identify and remove the effect of radio sources from the data (see Fig. 3).

The telescope observes in the band 12–18 GHz with cryostatically cooled NRAO indium-phosphide front-end amplifiers and fully-cooled feeds. The overall system tem-

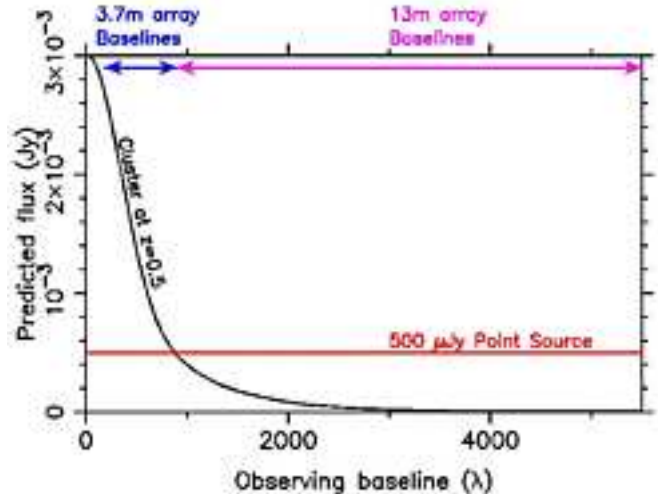


Fig. 3. Simulated plot of interferometer detected flux against observing baseline for a galaxy cluster at $z = 0.5$ and a point source (for convenience the absolute value of the negative S–Z flux is plotted). Since the cluster has large angular extent, its flux is quickly resolved out as the baseline length is increased whilst the flux from the point source is constant. The Small Array of 3.7-m dishes is therefore required to give access to the short baselines which detect the S–Z effect and the Large Array will measure the flux of any point sources in the field and allow their effects to be subtracted.

perature is approximately 25 K. We detect a single linear polarisation, measuring Stokes' parameter $I + Q$. The radio frequency is mixed with a 24-GHz local oscillator, downconverting to an intermediate frequency (IF) band of 6–12 GHz. Amplification, equalisation, path compensation and automatic gain control are then applied to the IF signal. The correlator is an analogue Fourier transform spectrometer with 16 correlations formed for each baseline at path delays spaced by 25 mm. Both '+' and '-' correlations (Thompson et al. 2001) are formed in this fashion by use of 0° and 180° hybrids respectively. From these, eight 0.75-GHz channels are synthesised.

4. Current status and commissioning results

Construction of the Small Array is now complete. Commissioning observations have detected SZ effects towards several known clusters. Figure 4 shows a 6 hour observation towards A773 after source subtraction; for comparison, Fig. 5 shows an image made from 460 hours of earlier RT data. These maps show significant detections of S–Z effects from both data sets, though the AMI map detects the outer regions of the cluster gas and so measures a higher integrated flux density. The RT resolves out most of the S–Z signal as one would expect from Fig. 3.

A longer observation of 34 hours was made towards the cluster A1914 (AMI Collaboration 2006) and the S–Z effect is detected with a significance of 17σ (Fig. 6). There is sufficient signal-to-noise in this observation to allow mapping of the S–Z effect in the separate frequency channels and this allows us to produce the spectrum shown

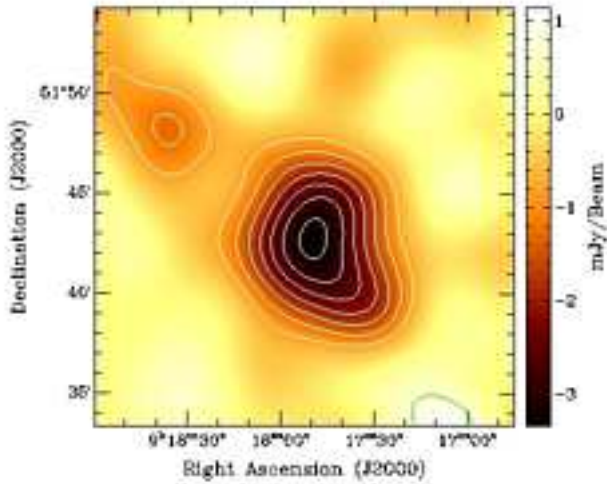


Fig. 4. AMI observation of the cluster A773 made from 6 hours of data.

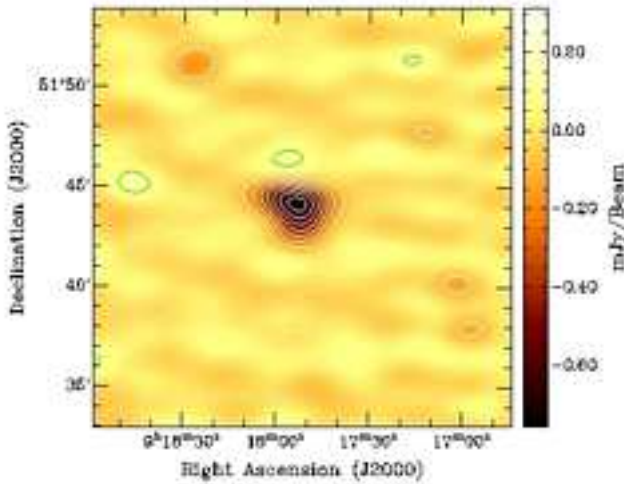


Fig. 5. RT observation of the cluster A773 made from 460 hours of data.

in Fig. 7. This shows that the decrement measured by AMI is consistent with an S-Z spectrum, which differs from a thermal spectrum by less than 0.5% between 13.5 and 18 GHz.

These commissioning observations give us confidence that the system is working and show that the Small Array sensitivity per channel is approximately $350 \text{ mJy s}^{-1/2}$, which is consistent with that assumed in our simulations (Kneissl et al. 2001). However, the deeper observations and calculations based on the 9C survey source counts (WalDRAM et al. 2003) show that the AMI maps presented here are limited by source confusion (Scheuer 1957) rather than thermal noise. This and the fact that we have had to remove 18 point sources from our data emphasise the importance of source subtraction, which for AMI will be provided by the Large Array.

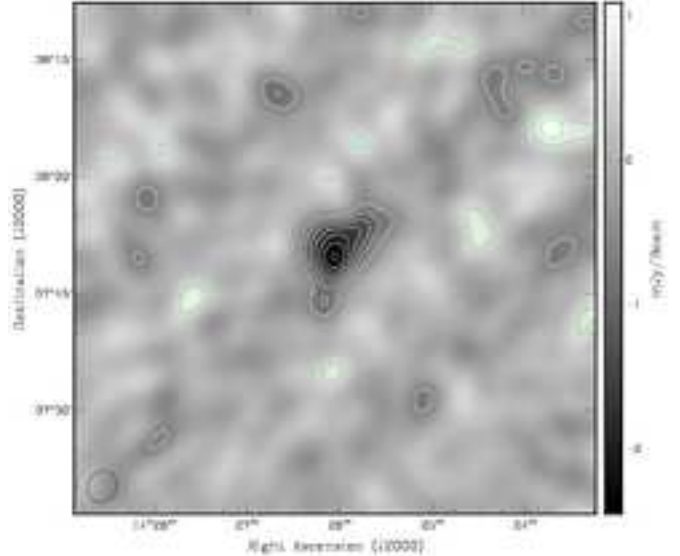


Fig. 6. CLEANED map of the S-Z effect in A1914 after subtraction of 18 sources. The integrated S-Z flux in the map is $-8.6 \pm 0.5 \text{ mJy}$ and the noise on the map is 0.19 mJy/beam .

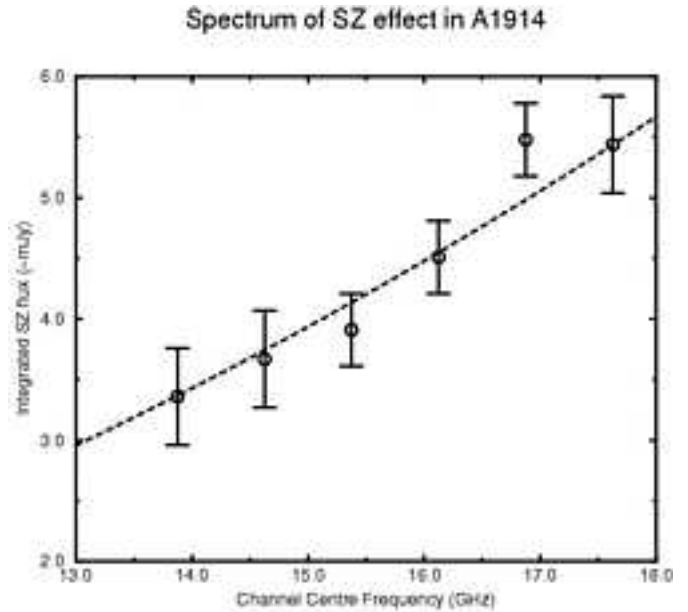


Fig. 7. Spectrum of the S-Z effect in A1914. The integrated flux is found over a 56 square arcminute region at the cluster centre. The magnitude of the negative S-Z flux is shown for convenience. The error bars are the 1σ errors from the channel maps which are dominated by source confusion; errors between different channels are therefore not independent. The dashed line shows a thermal spectrum ($\alpha = -2$ in the Rayleigh-Jeans region) constrained to pass through the 13.875 GHz point.

Observations with the RT have now been concluded. The three outlying antennas of the RT have been successfully moved to form a compact Large Array with the East-West array of five previously used for S-Z work. The upgrade of the feed-assembly, IF chain and correlator is now underway. These systems are essentially identical to those used on the Small Array, apart from the require-

ment for two further steps in the path compensator and additional amplification and equalisation because of the longer IF cables.

5. Future observing strategy

5.1. Pointed observations of known clusters

It will be necessary for AMI to calibrate the cluster scaling relations from pointed observations towards known clusters in order to be able to properly interpret the results of blind surveys. We have already started this programme with the Small Array, combining with source survey data from the RT. There are three main sub-samples of our first targets:

- NORAS: we have defined a sample from the NORAS (Böhringer et al. 2000) catalogue with ($L_X > 7 \times 10^{44} \text{ergs}^{-1}$, $z > 0.1$, $\delta > 30^\circ$) comprising 17 clusters. Combining with archive X-ray data we will also be able to calculate f_g and H_0 at low redshift.
- MACS: we have selected the 15 brightest ($L_X > 10^{45} \text{ergs}^{-1}$) clusters with redshift $z > 0.3$ from the Massive Cluster Survey (MACS Ebeling et al. 2001). By comparing with the NORAS samples we aim to constrain possible evolution in the cluster scaling relations.
- High-redshift: we plan to observe and confirm the increasing number of high-redshift clusters detected in other wavebands as they are reported in the literature.

5.2. Blind surveys

Before the completion of the Large Array we will be able to conduct surveys for clusters towards ten regions of $\approx 1 \text{ deg}^2$ which have already been surveyed by the RT as part of the VSA programme (Taylor et al. 2003). Once the Large Array becomes available we will begin wide and shallow surveys (six months over 100 deg^2), yielding massive lower redshift clusters and then narrow and deep ones (one year over 10 deg^2), yielding lower mass, higher redshift clusters. These will probe different regions of the cluster number density function. In addition, we will also survey the XMM Large Scale Structure Survey regions and other multi-wavelength deep fields. These observations will allow us to understand the selection function of different cluster-finding methods; a joint analysis will further provide information on cluster physics.

6. Acknowledgements

AMI is a project of the Cavendish Astrophysics Group and is supported by the Particle Physics and Astronomy Research Council.

References

AMI Collaboration, 2006, MNRAS, 369, L1

Bartlett J. G. & Silk J., 1994, ApJ 423, 12
 Bond J.R. & Meyers S.T., 1991, in: Trends in Astroparticle Physics, ed. Cline D., World Scientific, Singapore.
 Birkinshaw, M., 1999, Phys. Rep., 310, 97
 Birkinshaw, M. & Hughes, J. P., ApJ, 1994, 420, 33
 Böhringer, H., et al., 2000, ApJS, 129, 435
 Carlstrom, J. E., Holder, G. P., & Reese, E. D., 2002, ARA&A, 40, 643
 Ebeling, H., et al., 2001, ApJ, 553, 668.
 Grainge, K., et al., MNRAS, 1993, 265, L57
 Holzapfel, W. L., et al., ApJ, 481, 35
 Jones, M. E., 2002, ASPC, 257 in ‘AMiBA 2001: High- z Clusters, Missing Baryons, and CMB Polarization’, edited by Lin-Wen Chen, Chung-Pei Ma, Kin-Wang Ng, and Ue-Li Pen., ASPC, San Francisco, 257, 35
 Kneissl, R., et al., 2001, MNRAS, 328, 783
 Komatsu, E., et al., 1999, ApJ, 516, L1
 Korolev, V. A., Sunyaev, R. A., & Yakubtsev, L. A., 1986, Sov. Astron. Lett., 12, 141
 Kosowsky, A., 2003, NewAR, 47, 939
 Lancaster, K., et al., 2005, MNRAS, 359, 16
 Lo K., 2002, in ‘AMiBA 2001: High- z Clusters, Missing Baryons, and CMB Polarization’, edited by Lin-Wen Chen, Chung-Pei Ma, Kin-Wang Ng, and Ue-Li Pen. ASPC, San Francisco, 257, 3
 Holder, G. P., et al., 2000, ApJ, 544, 629
 Mohr, J. J., et al, 2003, NuPhS, 124, 63
 Myers, S. T., et al., 1997, ApJ, 485, 1
 Pointecouteau, E., et al., ApJ, 519, L115
 Reese E. D., Mohr Reese E. D., et al., ApJ, 2000, 533, 38
 Rosati, P., Borgani, S., & Norman, C., 2002, The Evolution of X-ray Clusters of Galaxies, ARAA, 40, 539
 Scheuer, P. A. G., 1957, PCPS, 53, 764
 Sunyaev, R. A. & Zel’dovich, Ya B., 1972, Comm. Astrophys. Sp. Phys., 4, 173
 Taylor, A., et al., 2003, MNRAS, 341, 1066
 Thompson, A. R., Moran J. M., & Swenson G. W., 2001, “Interferometry and Synthesis in Radio Astronomy”, pubs. John Wiley & Sons Inc.
 Udomprasert, P. S., Mason, B. S., Readhead, A. C. S., & Pearson T. J., 2004, ApJ, 615, 63
 Waldram E. M., et al., 2003, MNRAS, 342, 915